

Ab initio study of the properties of $\text{Ti}_{1-x-y}\text{Si}_x\text{Al}_y\text{N}$ solid solution

L. Marques^{*}, S. Carvalho, F. Vaz, M. M. D. Ramos, L. Rebuta

Centro de Física da Universidade do Minho, 4710-057, Braga, Portugal

Abstract

We have studied the electronic, structural, and elastic properties of $\text{Ti}_{1-x-y}\text{Si}_x\text{Al}_y\text{N}$ metastable phase, using first principles calculations based on the density functional theory. These calculations provide the lattice parameter, density of states, cohesive energy, formation energy and elastic constants, when Si and Al atoms replace Ti in the TiN lattice. The calculated values of lattice parameters and elastic constants are generally in good agreement with experiments and compare well with other theoretical results. We show that the trend followed by cohesive energy, formation energy, elastic constants is related to the electronic properties and bonding characteristics of these compounds.

Keywords: Titanium aluminum silicon nitride; hard coatings; magnetron sputtering; density functional theory

^{*} Corresponding author. Fax: +351253604061
Email address: lsam@fisica.uminho.pt

1. Introduction

Traditional transition metal hard wear-resistant coatings, played an important role in the development of cutting and forming tools. Increasing requirements on high speed and dry cutting applications open up new demands on the quality of the coating materials used. The alloying of TiN with small amounts of Al and or Si allows a great improvement of the characteristics TiN coatings, in terms of hardness and oxidation resistance, which led ternary/quaternary $Ti_{1-x-y}Si_xAl_yN$ systems to be considered as good alternatives to TiN in many industrial applications [1-10]. These coatings can be deposited by physical vapour deposition (PVD) techniques. When kinetics constraints due to low deposition temperature are present, and for low Si concentrations, a $Ti_{1-x-y}Si_xAl_yN$ metastable solid solution with fcc NaCl structure is formed where some Si and/or Al atoms are replacing Ti atoms in TiN fcc matrix [3-8].

Due to the importance of these type coatings, numerous experimental [1-10] and theoretical studies [11-13,21] have been conducted mainly on ternary systems, but there is little knowledge about the properties of quaternary $Ti_{1-x-y}Si_xAl_yN$ systems. The purpose of this work is to contribute to these studies by investigating the structural, electronic and elastic properties of the $Ti_{1-x-y}Si_xAl_yN$ fcc structures, using ab initio density functional theory calculations. The calculations provide insight into the theoretical lattice parameter, formation energy, cohesive energy, and elastic constants when Si and/or Al atoms replace some Ti atoms in TiN fcc lattice. The results of the present calculations are compared with experimental data obtained from a few selected samples prepared by magnetron sputtering, exhibiting a $Ti_{1-x-y}Si_xAl_yN$ metastable solid solution phase [10, 14-16]. We explain the trend followed by these parameters with the electronic properties and bonding characteristics of the quaternary systems.

2. Computational details

The first principles calculations were performed within the density functional theory [17] (DFT) formalism, using the Cambridge Serial Total Energy Package (CASTEP)[18]. It solves the Kohn-Sham equations with periodic boundary conditions and the pseudopotential method as an approximation of the atomic core – valence electron interaction, while the electronic wavefunctions are expanded in a plane wave basis. We adopted ultrasoft type pseudopotentials, due to its computational efficiency, and the generalized gradient density approximation of Perdew, Burke and Ernzerhof (GGA-PBE)[19] for the exchange-correlation functional, due to its accuracy in describing the bulk properties of many materials.

For the calculation of the ground state total energy, we used an eight atom cubic supercell with rock salt structure for the TiN, $\text{Ti}_{0.75}\text{Al}_{0.25}\text{N}$ and $\text{Ti}_{0.75}\text{Si}_{0.25}\text{N}$, while in the case of the quaternary $\text{Ti}_{1-x-y}\text{Si}_x\text{Al}_y\text{N}$ system a 32 atoms supercell was used. In order to study the effect of alloying TiN with Si and/or Al, the central titanium atoms in the supercells were replaced by Si, Al atoms. Because we just studied one particular arrangement of atoms for each alloy composition, our theoretical results do not correspond to properties of real $\text{Ti}_{1-x-y}\text{Si}_x\text{Al}_y\text{N}$ random alloys. However, the fact that our calculated density of states (DOS) is in good agreement with other calculations accounting for the disorder of TiAlN alloys [13], gives some reliability to our calculations and interpretation of the trends observed in experimental results.

The Brillouin zone was sampled with the Monkhorst-Pack scheme [20] using a k point $10 \times 10 \times 10$ mesh for the smaller supercells and a $3 \times 3 \times 6$ mesh for the 32 atoms supercells. A plane wave energy cutoff of 350 eV and an energy convergence limit of 5×10^{-7} eV/atom were used in total energy calculations, guaranteeing a high level of convergence. The geometry of the resulting structures was fully optimized using the

Broyden-Fletcher-Goldfarb-Shanno (BFGS) minimization technique with the following tolerances: residual force less than 0.01 eV/Å, and residual bulk stress less than 0.02 GPa.

Using the calculation procedure describe above, we obtained the total energies for the various $\text{Ti}_{1-x-y}\text{Si}_x\text{Al}_y\text{N}$ structures, together with total energy of crystalline titanium (hcp), aluminium (hcp), silicon (diamond cubic) and molecular nitrogen. The formation (E_{form}) energy was then calculated by

$$E_{\text{form}}(\text{Ti}_{(1-x-y)}\text{Si}_y\text{Al}_x\text{N}) = E_{\text{tot}}(\text{Ti}_{(1-x-y)}\text{Si}_y\text{Al}_x\text{N}) - 0.5 \cdot [(1-x-y) \cdot E_{\text{tot}}(\text{Ti}^{\text{hcp}}) + x \cdot E_{\text{tot}}(\text{Al}^{\text{hcp}}) + y \cdot E_{\text{tot}}(\text{Si}^{\text{cub}}) + 0.5 \cdot E_{\text{tot}}(\text{N}_2)]. \quad (1)$$

The cohesive energy (E_{coh}) was calculated in the usual way from the difference in total energy between the isolated atoms and the (Ti,Si,Al)N compound,

$$E_{\text{coh}}(\text{Ti}_{(1-x-y)}\text{Si}_y\text{Al}_x\text{N}) = 0.5 \cdot [(1-x-y) \cdot E_{\text{tot}}(\text{Ti}) + x \cdot E_{\text{tot}}(\text{Al}) + y \cdot E_{\text{tot}}(\text{Si}) + E_{\text{tot}}(\text{N})] - E_{\text{tot}}(\text{Ti}_{(1-x-y)}\text{Si}_y\text{Al}_x\text{N}). \quad (2)$$

The elastic constants were calculated for each structure by applying suitable lattice distortions to the relaxed cubic structure. The elastic moduli were obtained from the elastic constants using the voight approximation for polycrystalline materials [21].

3. Results and discussion

The XRD experiments of the selected samples, exhibiting a $\text{Ti}_{1-x-y}\text{Si}_x\text{Al}_y\text{N}$ metastable solid solution phase, are illustrated in figure 1. Previously, we have already discussed the developed structure [10,14,15]. Nevertheless, for the sake of clarity some features should be pointed out. Figure 1 suggests the presence of phases with a fcc structure, similar to TiN. For the particular case of $\text{Ti}_{0.65}\text{Al}_{0.35}\text{N}$ sample a lattice parameter of 0.423 nm was derived using the $\text{sen}^2\Psi$ method. In the case of the $\text{Ti}_{0.5}\text{Si}_{0.13}\text{Al}_{0.37}\text{N}$ sample, the introduction of a small silicon percentage further reduces the lattice parameter to a value of 0.417 nm. These results justify the assumption that the observed

decrease in the lattice parameter must be associated with the fact that Si and Al atoms substitute Ti atoms, while still remaining a fcc structure.

Figure 2 shows a comparison of the total DOS of TiN, $\text{Ti}_{0.75}\text{Si}_{0.25}\text{N}$, $\text{Ti}_{0.75}\text{Al}_{0.25}\text{N}$, $\text{Ti}_{0.69}\text{Si}_{0.06}\text{Al}_{0.25}\text{N}$ compounds, putting in evidence the effect of Ti substitution by Si, Al atoms on the DOS. The total DOS for TiN, is in good agreement with previous calculations [23]. The band between -2.5 eV and -11 eV consists of a mixture of Ti 3d and N 2p states and is responsible for the covalent bonding in TiN. The calculated DOS of $\text{Ti}_{0.75}\text{Al}_{0.25}\text{N}$ is also in good agreement previous calculations accounting for the disorder of these alloys [13]. Notice the appearance on top valence band of $\text{Ti}_{0.75}\text{Si}_{0.25}\text{N}$ and $\text{Ti}_{0.75}\text{Al}_{0.25}\text{N}$ compounds of a small peak around -4 eV, due to Si, Al p states, which corresponds to the covalent interaction between Ti, Si, Al and N atoms. The addition of Si, Al introduces new p states competing with existing N 2p states for Ti 3d electrons, thus weakening Ti-N atomic bonding and explaining the observed decrease of formation and cohesive energies with Si, Al addition to TiN lattice. This bond weakening is stronger for Si, because each Si atom has more p electrons competing for Ti 3d electrons. The Fermi level lies within a sharply increasing peak, essentially made up of Ti 3d states, revealing that the metallic bonding plays a major role in determining the properties of these compounds.

Table 1 shows the calculated formation energy, cohesive energy for the various $\text{Ti}_{1-x-y}\text{Si}_x\text{Al}_y\text{N}$ structures. The calculations overestimate the formation and cohesive energy for TiN, relative to experiments ($E_{\text{formation}} = -1.73$ eV/atom; $E_{\text{cohesive}} = -6.9$ eV/atom), which can be attributed to systematic errors in the description of the exchange–correlation term and/or to an improper accounting of the groundstate of isolated atoms [22]. The calculations predict that all the structures studied here are stable, with TiN being the most stable of all because of its higher formation energy. The substitution of Ti atoms by Si, Al atoms reduces the formation energy, suggesting that the

ternary/quaternary compounds exist in a metastable phase. The same trend is observed for cohesive energy, which indicates a weakening of the atomic bonding with the addition of Si, Al to TiN lattices.

We have also analyzed the properties of bonding between atoms through Mulliken analysis of the overlap population of nearest - neighbours, which is used to indicate the degree of covalency in materials. A large value for this population indicates that the two atoms in question are bonded, while a negative value means that the atoms are in an antibonded state. A value close to zero indicates that there is no significant interaction between the electronic populations of the two atoms. Table 2 lists the calculated Mulliken populations and bond lengths for the $Ti_{1-x-y}Si_xAl_yN$ compounds. The substitution of Ti by Si, Al reduces the Mulliken population of Ti-N bonds compared to that of TiN, meaning that the degree of covalency of Ti-N bonds is weaker for $Ti_{1-x-y}Si_xAl_yN$ compounds and explaining the general decrease of cohesive energy. The weak Si-N binding compared to Al-N, justifies the lower cohesion energy of $Ti_{0.75}Si_{0.25}N$ relatively to $Ti_{0.75}Al_{0.25}N$.

Table 3 lists the calculated lattice parameters and elastic constants of $Ti_{1-x-y}Si_xAl_yN$ structures, together with results of other theoretical [21] and previous experimental studies [14,16,24]. The calculated lattice parameters for $Ti_{1-x-y}Si_xAl_yN$ structures, are in good agreement with experimental stress free lattice parameters. The decrease of the lattice parameter with substitution of Ti atoms by Si and or Al atoms is due to the lower atomic radius of these atoms and in case of Al also to the decrease of the electrostatic repulsion between atoms compared to Ti, due to its lower number of valence electrons. The calculated elastic parameters are in good agreement with other theoretical, thus ensuring its reliability. The alloying of TiN with Si leads to a strong decrease of all calculated elastic constants, in good agreement with the experimental results. This can be explained by the weakening of Ti-N bonding. The same reason also explains the

general decrease of elastic parameters observed in case of TiAlN, except for the trigonal shear modulus (C_{44}), which increases in agreement with the experimental data. According to ref 25, this fact is related to the decrease of number of free electrons, since Al has one valence electron less than Ti, thus contributing to depopulate the metallic bands close to the Fermi level, which are very sensitive to shear strain and give a negative contribution to C_{44} . The addition of a small quantity of silicon to $Ti_{0.75}Al_{0.25}N$ results in an increase of C_{44} and in elastic moduli, in agreement with the trend observed experimentally. This is probably related to the depopulation of metallic bands close to the Fermi level, due to the reduction of number of Ti 3d electrons when Ti is replaced by Si in the matrix.

4. Conclusions

We studied the electronic, structural and mechanical properties of $Ti_{1-x-y}Si_xAl_yN$ structures, using an ab-initio approach based on DFT and the pseudo potential method. Although our theoretical results do not correspond to properties of real $Ti_{1-x-y}Si_xAl_yN$ random alloys, they show important trends and provide a physical interpretation of experimental data. The calculated the lattice parameters are in good agreement with the trend observed experimentally, supporting the fact that a solid solution is created when replacing some Ti atoms by Si and Al atoms. We found that the alloying of TiN with Si, Al leads to a general decrease of cohesive, formation energy and elastic constants, which we relate with the weakening of TiN binding. Our theoretical results reproduce the experimental trend followed by elastic constants with substitution of Ti by Si, Al atoms. We attribute the increase of trigonal shear modulus with addition of Al, and small quantities of Si, to the depopulation of the metallic bands close to Fermi level, which are very sensitive to shear strain.

Acknowledgements

We would like to acknowledge to Prof. Marshall Stoneham and UCL for let us use the CASTEP software.

References

- [1] Veprěk S, Reiprich S. *Thin Solid Films* 1995;268: 64.
- [2] Veprek S., Männling H.-D., Jilek M., Holubar P., *Mat. Sci Eng A* 2004; 366, 202-205.
- [3] Vaz F, Rebouta L, Ramos S, Silva M. F, Soares J. C. *Surf. Coat. Technol.* 1998; 108-109: 236.
- [4] Meng W. J, Zhang X. D, Shi B, Tittsworth R. C, Rehn L. E, Baldo P. M, *J. Mater. Res.* 2002; 17: 2628.
- [5] Nose M, Chiou W. A, Zhou M, Mãe T, Meshii M. *J. Vac. Sci. Technol. A* 2002; 20: 823.
- [6] Flink A, Larsson T, Sjöblén J, Kralsson L, Hultman L. *Surf. Coat. Technol.* 2005; 200: 1535.
- [7] Tanaka Y, Ichimiya N, Onischi Y, Yamada Y. *Surf. Coat. Technol.* 2001; 146-147: 215.
- [8] Ribeiro E., A. Malczyk A., Carvalho S., Rebouta L., Fernandes J.V., Alves E., Miranda A.S. *Surf. Coat. Technol.* 2002; 151-152: 515.
- [9] Vaz F, Rebouta L, Goudeau Ph. *Thin Solid Films* 2002; 402: 195.
- [10] Ribeiro E, Rebouta L, Carvalho S, Vaz F, Fuentes G. G, Rodriguez R, Zazpe M, Alves E, Goudeau Ph, Rivière J. P. *Surf. Coat. Technol.* 2004; 188-189: 351.
- [11] Zhang R. F, Veprěk S. *Mater. Sci. Eng. A*, 2007; 448: 111.
- [12] Podgursky V. J. *Phys. D: Appl. Phys.* 2007; 40: 4021.
- [13] Alling B, Ruban A. V, Karimi A, Peil O. E, Simak S. I, Hultman L, Abrikosov I. *Phys. Rev. B*, 2007; 75: 045123.
- [14] Carvalho S, Ribeiro E, Rebouta L, Vaz F, Alves E, Schneider D, Cavaleiro A *Surf. Coat. Technol.* 2003; 174-175: 984.
- [15] Carvalho S., Ribeiro E., Rebouta L., Pacaud J., Goudeau Ph., Renault P.O., Rivière J.P., Tavares C.J. *Surf. Coat. Technol.* 2003; 172: 109.
- [16] Carvalho S, Vaz F, Rebouta L, Schneider D, Cavaleiro A, Alves E. *Surf. Coat. Technol.* 2001, 142-144: 110.
- [17] Kohn W, Sham L. *J. Phys. Rev A* 1965; 140: 1133.
- [18] Segall M, Lindan P, Probert M, Pickard C, Hasnip P, Clark S, Payne M, *J. Phys.: Condens. Matter* 2002, 14: 2717.

- [19] Perdew J. P, Burke K, Ernzerhof M. Phys. Rev. Lett. 1996; 77: 3865.
- [20] Monkhorst J. H, Pack J Phys. Rev. B 1976; 13: 5188.
- [21] Chen K, Zhao L. R, Rodgers J, Tse J.S. J. Phys. D: Appl. Phys 2003; 36: 2725.
- [22] Arya A, Carter E. A. J. Chem. Phys. 2003; 118: 8982.
- [23] Ahuja R, Eriksson O, Wills J. M, Johansson B. Phys. Rev B 1996; 53: 3072.
- [24] Kim J. O, Achenbach J. D, Mirkarimi P. B, Shinn M, Barnett S. A. J. Appl. Phys. 1992; 72: 1805.
- [25] Jhi S, Ihm J, Louie S. G, Cohen M. L. Nature 1999; 399: 132.

Figure captions

Fig. 1: XRD patterns for different samples: a) $\text{Ti}_{0.8}\text{Si}_{0.2}\text{N}$ b) $\text{Ti}_{0.5}\text{Al}_{0.37}\text{N}$ c) $\text{Ti}_{0.65}\text{Si}_{0.13}\text{Al}_{0.35}\text{N}$.

Fig. 2: Calculated total density of states: TiN DOS (dotted line), $\text{Ti}_{0.75}\text{Al}_{0.25}\text{N}$ DOS (full line), $\text{Ti}_{0.75}\text{Si}_{0.25}\text{N}$ DOS (dashed line). The Fermi energy (ϵ_F) is set at zero energy and is marked by vertical line.

Table 1 Results from calculations of cohesive energy (E_{coh}) and formation energy (E_{form}) for $Ti_{1-x-y}Si_xAl_yN$ structures.

Compound	E_{form} (eV/atom)	E_{coh} (eV/atom)
TiN	-2.72	-9.44
$Ti_{0.75}Al_{0.25}N$	-2.48	-8.83
$Ti_{0.69}Si_{0.06}Al_{0.25}N$	-2.37	-8.68
$Ti_{0.75}Si_{0.25}N$	-2.12	-8.66

Table 2 Calculated Mulliken populations and bond lengths of nearest neighbours for $Ti_{1-x-y}Si_xAl_yN$ structures.

Bond	TiN		Ti_{0.75}Al_{0.25}N		Ti_{0.75}Si_{0.25}N		Ti_{0.69}Si_{0.06}Al_{0.25}N	
	Population	Length (Å)	Population	Length (Å)	Population	Length (Å)	Population	Length (Å)
Ti - N	1.67	2.12	0.6- 0.93	2.1	0.59-0.96	2.11	0.25-0.77	2.02 -2.28
Al - N	-	-	0.74	2.1	-	-	0.35-0.65	2.09 -2.10
Si - N	-	-	-	-	0.36	2.11	0.51-0.59	1.91-2.09

Table 3 Results from calculations and measurements of lattice parameter (a_0), bulk modulus (B), shear modulus (G), Young's modulus (E), tetragonal shear modulus (C_{11} - C_{12}), trigonal shear modulus (C_{44}) and C_{11} elastic constant for $Ti_{1-x-y}Si_xAl_yN$ structures, compared with other calculated and experimental data.

Compound	a_0 (nm)	C_{11} (GPa)	$C_{11}-C_{12}$ (GPa)	C_{44} (GPa)	B (GPa)	G (GPa)	E (GPa)
TiN	0.424	615	484	172	292	226	539
$Ti_{0.75}Al_{0.25}N$	0.420	503	349	183	270	180	441
$Ti_{0.69}Si_{0.06}Al_{0.25}N$	0.418	496	325	227	279	201	487
$Ti_{0.75}Si_{0.25}N$	0.423	438	304	94	235	117	302
Other calculations [21]							
TiN	0.424	671	565	166	295	203	514
$Ti_{0.75}Al_{0.25}N$	0.422	504	361	174	257	179	435
Experimental							
TiN [24]	0.424	625	460	163	318	190	475
$Ti_{0.65}Al_{0.35}N$ [14]	0.423 ^b	474	348	174	242	174	421
$Ti_{0.50}Si_{0.13}Al_{0.37}N$ [14]	0.417 ^b	525	385	193	268	193	466
$Ti_{0.8}Si_{0.2}N$ [3]	0.418 ^a	293	215	107	150	103	260

^aLattice parameters measurements by XRD.

^bLattice parameters measurements by $\sin^2\psi$ method.

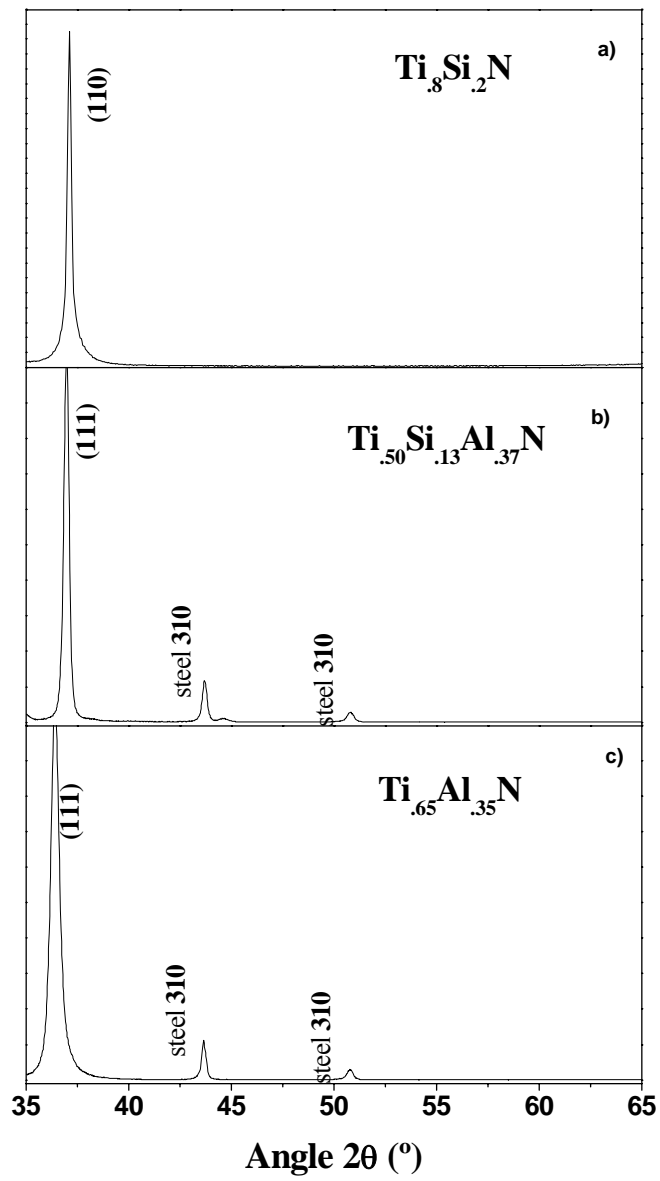


Figure 1

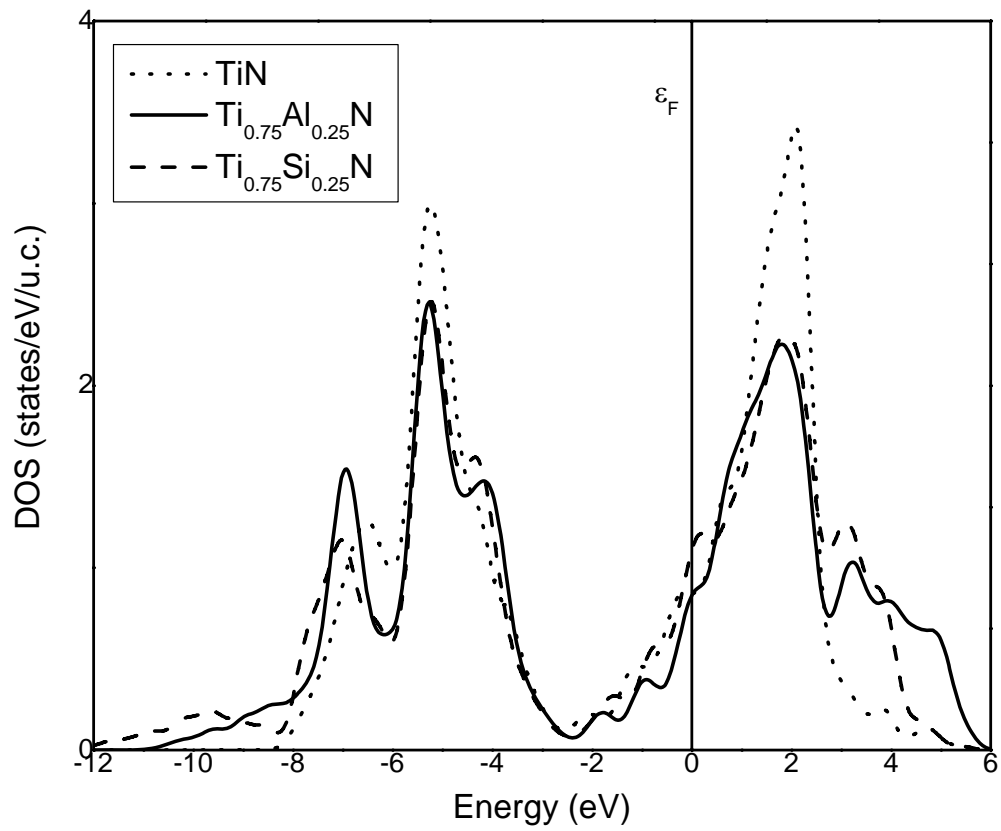


Figure 2